Original Article

cGAS-STING pathway expression as a prognostic tool in NSCLC

Kristine Raaby Gammelgaard[1#], Birgitte Sandfeld-Paulsen[2#], Stine Høvring Godsk[1], Christina Demuth[2], Peter Meldgaard[3], Boe Sandahl Sorensen[2], Martin Roelsgaard Jakobsen[1]

[1]Department of Biomedicine, Aarhus University, Aarhus, Denmark; [2]Department of Clinical Biochemistry, Aarhus University Hospital, Aarhus, Denmark; [3]Department of Oncology, Aarhus University Hospital, Aarhus, Denmark

Contributions: (I) Conception and design: K Raaby Gammelgaard, B Sandfeld-Paulsen, BS Sorensen, MR Jakobsen; (II) Administrative support: MR Jakobsen, BS Sorensen; (III) Provision of study materials and patient's: K Raaby Gammelgaard; B Sandfeld-Paulsen, BS Sorensen, P Meldgaard; (IV) Collection and assembly of data: K Raaby Gammelgaard, B Sandfeld-Paulsen, C Demuth, SH Godsk; (V) Data analysis and interpretation: K Raaby Gammelgaard, B Sandfeld-Paulsen, C Demuth, MR Jakobsen; (VI) Manuscript writing: All authors; (VII) Final approval of manuscript: All authors.

[#]These authors contributed equally to this work.

Correspondence to: Kristine Raaby Gammelgaard; Martin Roelsgaard Jakobsen. Department of Biomedicine, Aarhus University, Høegh-Guldbergs Gade 10 bld. 1115-220, DK-8000 Aarhus C, Denmark. Email: kraaby@biomed.au.dk; mrj@biomed.au.dk.

Background: Disease recurrence in localized lung adenocarcinoma is a major obstacle for improving the overall outcome of lung cancer. Thus, better prognostic biomarkers are needed to identify patients at risk. In order to clear cancer, immune detection of tumor cells is of vital importance. DNA-leakage into the cytosol and tumor environment is one important tumor-associated danger signal and cGAS is a pivotal DNA-sensor that detects misplaced DNA and initiates an innate immune response. In this study, we investigate the cGAS-STING-pathway expression in tumor tissue and circulating immune cells from lung adenocarcinoma patients in relation to stage of disease and overall survival (OS).

Methods: Gene expression was measured using target specific droplet digital polymerase chain reaction (ddPCR) assays in a cohort of 80 patients with lung adenocarcinoma and 45 patients suspected of lung cancer, but determined to be cancer-free. The expression values were correlated to stage of disease. For further exploration of stage dependent expression, we used a publicly available gene expression data set to stratify patients by stage and correlate gene expression to OS.

Results: In both tumor tissue and peripheral blood mononuclear cells (PBMCs) from cancer patients, we observed differential expression of cGAS-STING pathway components compared to cancer-free individuals. Furthermore, cGAS-STING pathway expression was elevated in PBMCs from patients with localized disease (stage I and II) compared to patients with metastatic disease (stage III and IV). Survival analysis based on publicly available gene expression data sets demonstrated a superior OS for patients with localized disease and high levels of *cGAS*, *STING* and *TBK1*.

Conclusions: The expression of the cGAS-STING pathway is stage dependent and high expression is correlated with localized adenocarcinoma. For patients with localized disease, high *cGAS*, *STING* and *TBK1* expression correlated with improved OS and may be a potential biomarker for this patient subgroup.

Keywords: Non-small cell lung cancer (NSCLC); immuno-oncology; adenocarcinoma; innate immune system; STING

Submitted Apr 03, 2020. Accepted for publication Sep 19, 2020.
doi: 10.21037/tlcr-20-524
View this article at: http://dx.doi.org/10.21037/tlcr-20-524

Introduction

The immune system is indispensable for combatting cancer and constitutes a challenge for the cancer to overcome. Downregulation of neoantigens is an example of a key-mechanism of avoiding the immune system. In a recent study, it was highlighted how localized lung cancer over time selectively diminish neoantigens detected by the immune system and escape an immune response (1). Modulating the immune response is not only an essential step for cancer growth to progress, but it also constitutes a major obstacle for anti-cancer therapy response. Several studies indicate the importance of a functional immune system by demonstrating the correlation of T-cell activation and antigen presentation capacity (2-4) with response to anti-cancer therapy. Hence, a functional immune system is a determining factor for preventing progression as well as predicting prognosis in many types of cancer, including lung cancer.

The 5-year overall survival (OS) rate for lung cancer is approximately 18%, and although localized disease has a better prognosis with a 5-year OS of 55%, it remains a highly deadly disease (5). Despite curative resection, 30–55% of patients with localized disease develop recurrence and eventually die (6). The high risk of relapse in localized disease calls for better prognostic biomarkers to identify patients that may benefit from adjuvant treatment (7) or targeted therapy such as immune-checkpoint inhibitors (8).

To date, most studies in non-small cell lung cancer (NSCLC) have focused on the prognostic value of markers related to the adaptive immune system including expression of check-point molecules such as CTLA-4 on the immune cells and PD-L1 on tumor cells or infiltration of specific subsets of tumor-infiltrating lymphocytes (7,9). Yet, a functioning innate immune system is required for activation of the adaptive immune system. The significance of innate immune activity was illustrated in a RNA-microarray study of 432 lung adenocarcinoma patients with stage I–III disease. Here it was reported that several immune pathways were correlated with superior survival and 17 genes with specific importance for recurrence was identified (9,10). Interestingly, many of these genes encode chemokines and chemokine receptors responsible for recruiting innate immune cells, including macrophages and dendritic cells, critical for an effective immune response (9,11).

The innate immune system is activated through detection of aberrant molecules present within or outside the cells through specific pattern recognition receptors. One such example is sensors detecting DNA engulfed by antigen-presenting cells, or misplaced cytosolic DNA within the cancer cell itself that occurs by defects in DNA damage response mechanisms (12).

The cyclic GMP-AMP synthase (cGAS) is the pivotal DNA-sensor expressed within most tissues. Upon DNA binding the small agonist cyclic-AMP-GMP-nucleotide cGAMP is synthesized. cGAMP then binds to the adaptor protein stimulator of interferon genes (STING) (13) that subsequently activates tank binding kinase 1 (TBK1) leading to downstream activation of interferon regulatory factor 3 (IRF3) ensuing a type I interferon (IFN I) and cytokine response (14). Autocrine and paracrine IFN I signaling leads to transcription of interferon stimulated genes (ISGs) including chemokines and chemokine receptors leading to attraction and activation of innate immune cells and subsequent activation of the adaptive immune system. IFN I may, however, also induce transcription of proapoptotic genes (15).

Since, Aberrant DNA is especially abundant in cancer due to release from necrotic cells and through DNA-leakage into the cytosol of the cancer cells (16), cGAS signaling could potentially lead to IFN I production, immune activation and apoptosis of the cancer cell. Hence, downregulation of the cGAS-STING pathway constitutes a possible immune escape mechanism for cancer cells.

Studies on the cGAS-STING pathway expression in cancer illustrate an antitumor role and selective downregulation of one or multiple factors in the cGAS-STING pathway in tumor samples compared to normal samples in colorectal cancer, malignant melanoma, gastric cancer and hepatocellular carcinoma has been reported (17-20). Within a colorectal cancer cohort, high *cGAS* expression was shown to correlate with early-stage disease (17), and high *STING* expression has been reported to be an independent marker for a better prognosis in hepatocellular carcinoma for both early and advanced stages (19). *In vivo*, increased STING-activity induced by STING agonists initiates anti-tumoral responses both alone or in combination with check-point inhibitors (21-23). However, increased *STING* expression in HPV positive tongue squamous cell carcinoma followed by immunosuppression has also been reported (24). In addition, increasing levels of chromatin instability led to STING promoted tumor metastasis in a murine breast cancer model, resembling advanced stage disease (16). These contradictory findings outline a cancer type and possibly stage dependent function of STING.

Former investigations have explored the cGAS-STING pathway in relation to OS in lung cancer but no studies have taken disease stage into account. In an analysis of *STING* (*TMEM173*) and *cGAS* (*MB21D1*) expression across all stages of lung adenocarcinoma, they found a correlation between low gene expression and inferior survival (25). In addition, a recent study found that STING pathway activation, and especially *cGAS*, *CCL5* and *CXCL10* expression, is correlated with a favorable outcome to chemoimmunotherapy treatment (26). These studies highlight the potential key-role of the cGAS-STING pathway in relation to immune activation in lung cancer and further implies a possible prognostic value of this essential DNA-sensing pathway that needs further exploration.

Most studies so far, have merely focused on cGAS-STING pathway expression within the tumor tissue. Yet, Cassetta *et al.* recently showed a change in the transcriptional profile of circulating monocytes in patients with endometrial and breast cancer supporting the potential for gene expression studies based on circulating immune cells (27).

In the present study, we explore the cGAS-STING pathway in both lung cancer cell lines, and in tumor tissue biopsies and peripheral blood mononuclear cells (PBMCs) across all stages of disease with the purpose of evaluating the prognostic value of cGAS-STING pathway expression. In addition to the cGAS-STING pathway described, we also include IFI16 recently shown to have significant impact on the innate immune responses in human macrophages and keratinocytes (28). We present the following article in accordance with the REMARK reporting checklist (available at http://dx.doi.org/10.21037/tlcr-20-524).

Methods

Cell culture

All cell lines were purchased at ATCC (ATCC/LCG, Wesel, Germany) except PC9 (PHE culture collection, Salisbury, UK). Cells were grown in RPMI or DMEM according to supplied instructions supplemented with 10% fetal calf serum, 1% L-Glutamine and 1% penicillin-streptomycin (Gibco, Thermo Fischer Scientific, Waltham, MA, USA). The cells were grown at 37 ℃ and 5% CO_2.

Western blot analysis

Samples were harvested in RIPA buffer supplemented with protease and phosphatase inhibitor (Thermo Fisher Scientific, Waltham, MA, USA, cat. no. A32961) and 10 mM NaF (VWR, Søborg, DK, cat. no. J60251.AE). Before loading, the samples were mixed 1:1 with 2X Laemmli buffer (Sigma Aldrich, St. Louis, MO, USA, cat. no. 38733) and boiled at 95 ℃ for 3 min. The samples were loaded on a 10% Criterion™ TGX™ Precast Midi Protein Gel, 26 well (Bio-Rad Hercules, CA, USA, cat. no. 567-1035). The gel was blotted onto a Turbo Transfer Midi PVDF membrane (Bio-Rad Hercules, CA, USA, cat. no. 170-4157) and the membrane was blocked with 5% skimmed milk. The membrane incubated with primary antibody with rotation ON at 4 ℃, and hereafter incubated with secondary antibody for 1 h before development with ECL, SuperSignal West Dura Extended Duration Substrate (Bio-Rad Hercules, CA, USA, cat. no. 1705060) using the ImageQuant LAS 4000 system (GE Healthcare Life Sciences, Little Chalfont, UK). Antibody information: primary antibodies all used in ratio 1:1,000: Cell Signaling Technology (Danvers, MA, USA): anti-TBK1 cat. no. 3313 (84 kDa), anti-STING cat. no. 13647 (33–35 kDa), anti-cGAS cat. no. 15102 (62 kDa), anti-IRF3 (55 kDa) cat. no. 4302. Santa Cruz Biotechnology: anti-IFI16 cat. no. 8023 (88–98 kDa). Secondary antibodies: Peroxidase-AffiniPure F(ab')2 Fragment Donkey Anti-Rabbit IgG cat. no. 711-036-152, Peroxidase-AffiniPure F(ab')2 Fragment Donkey Anti-Mouse IgG cat. no. 715-036-150 (Jackson ImmunoResearch).

Transfection

Sixty thousand cells in a total volume of 500 µL media were seeded 1 day prior to transfection in Nunc 24-well plates. Lipofectamine® 2000 (Invitrogen, San Diego, CA, USA) was used for transfection with 2 µg/mL double stranded herring testis DNA (HT-DNA) (Sigma-Aldrich, St. Louis, MO, USA) or 40 ng/mL polyinosinic-polycytidylic acid (Poly I:C)-LMW (Invivogen, cat. no. tlrl-picw) according to the manufacturer's instructions.

IFN I measurement

Twenty hours after transfection, IFN I production was measured using a biofunctional Human HEK-Blue IFN-α/β reporter cell assay (Invivogen, San Diego, CA, USA). Fifty microliters of standard [IFN-α standard curve starting at 1,000 U/mL (PBL Assay Science, Piscataway, NJ, USA)] or supernatants from the stimulated cells were added to the

HEK-Blue IFN-α/β reporter cells and left ON. Supernatant (20 µL) from HEK-Blue IFN-α/β reporter cells were then mixed with 180 µL QUANTI-blue (Invivogen, San Diego, CA, USA) and the optical density at 620 nm was determined using a microplate reader to determine final concentration as unit/mL.

ELISA

CCL5/RANTES was detected using Human CCL5 DuoSet ELISA (R&D systems, cat. no. DY278) according to the manufacturer's instructions. The optical density was determined using a microplate reader set to 450 and 570 nm. The readings at 570 nm were subtracted from the 450 nm-reading to correct for optical imperfections in the plate.

Multiplex ELISA

Multiplex ELISA was performed using Meso Scale Discovery (MSD) U-plex platform according to manufacturer's protocol (cat. no. K15067L-2).

Ethical statement

The study was conducted in accordance with the declaration of Helsinki (as revised in 2013). The study was approved by The Central Denmark Region Committees on Biomedical Research Ethics (M-20100246) and the Danish Agency of Data Protection (1-16-02-346-14). All patients gave informed written consent before inclusion and individual consent for this retrospective analysis was waived.

Patient cohort

Patients were selected from a cohort of patients suspected of lung cancer and referred to the Department of Pulmonary Medicine, Aarhus University Hospital, Denmark between April 2011 and June 2015. For the original cohort the inclusion criteria were (I) age ≥18 years, (II) the patient had to sign a written informed consent. The only exclusion criterion was the presence of a current cancer. A total of 1,921 patients were included. At time of inclusion a blood sample was collected. If the diagnostic work-up led to a fine-needle aspiration (FNA), a small part of the diagnostic biopsy was obtained and further processed as described below in the RNA purification section. The cohort has been utilized for studies on the epidermal growth factor system, exosome analyses and comorbidity evaluations (29-34). In this present study, we retrospectively selected 80 patients with lung adenocarcinoma and 45 patients suspected of lung cancer, but diagnosed to be cancer-free. Patients were selected if matched pre-diagnostic blood and/or tissue were available. Patients with other cancer types (including other lung cancer subtypes) were excluded. Tumor biopsies, non-cancer biopsies and blood samples used for PBMC analysis for each patient was taken within a period of 14 days. To explore the prognostic value of clinical data and gene expression data from lung adenocarcinoma tumor tissue from the KMplot.com (35) (see methods) were employed. Patients were stratified by the median gene expression, cancer, stage and OS were employed as clinical endpoints.

RNA purification

Cell lines

RNA was purified using RNeasy mini kit (Qiagen, Hilden, Germany) on the QIACube instrument (Qiagen, Hilden, Germany) and eluted in 30 µL RNase-free water. One µg of RNA was used for cDNA synthesis using the iScript cDNA synthesis kit (Bio-Rad Hercules, CA, USA).

Tissue samples

Fine needle biopsies were obtained by FNAs, endoscopic ultrasound FNA (EUS-FNA) and/or endobronchial ultrasound guided transbronchial needle aspiration (EBUS-TBNA). RNA was purified using RNeasy micro kit (Qiagen, Hilden, Germany) on the QIACube instrument (Qiagen, Hilden, Germany) and eluted in 14 µL RNase-free water. Seven µL of RNA was used for cDNA synthesis using the iScript cDNA synthesis kit (Bio-Rad Hercules, CA, USA).

PMBCs

The PBMCs were isolated from a pre-diagnostic EDTA blood sample and stored at –80 ℃ until use. For RNA isolation, the PMBCs were transferred to 5 mL RNA protect (Qiagen, Hilden, Germany) and centrifuged for 5 min at 3,000 rcf. After removing the supernatant, 2 mL erythrocyte lysis buffer (Qiagen, Hilden, Germany) was added and left to incubate for 20 min on ice with frequent vortexing. The samples were centrifuged for 10 min at 4 ℃ and 400 rcf. The supernatant was removed, and the pellet dissolved in PBS and divided into two parts. The part for RNA was centrifuged, and the pellet dissolved in 350 µL RLT buffer and RNA purified using RNeasy mini kit and the QIAcube instrument. The RNA was eluted in 30 µL

of RNase-free water. Two hundred ng RNA was used for cDNA synthesis using the iScript cDNA synthesis kit (Bio-Rad, Hercules, CA, USA).

Droplet digital polymerase chain reaction (ddPCR)

Gene expression was analyzed using ddPCR. Measurements were set up on the QX200 droplet digital PCR system (Bio-Rad Hercules, CA, USA) with commercially available Taqman assays (Thermo Fisher Scientific, Waltham, MA, USA): ACTB (Hs03023943_g1), STING/TMEM173 (Hs00736955_g1) IFI16 (Hs00986757_m1), cGAS/MB21D1 (Hs00403553_m1), IRF3 (Hs00155574_m1), TBK1 (Hs00179410_m1). Actin was used as reference gene based on prior analysis (36). Reactions contained 5 µL cDNA, 1 µL of each primer-probe mix, and 10 µL 2× ddPCR Supermix for probes and 3 µL H_2O (Bio-Rad Hercules, CA, USA). For PBMCs and cell lines the cDNA concentration was adjusted to 0.2 ng/µL. The cycling steps for the ddPCR were as follows: 95 ℃ for 10 min, 40 cycles of 94 ℃ for 30 s, and 60 ℃ for 1 min, and finally 98 ℃ for 10 min. The ddPCR reactions were performed according to manufacturer's recommendations, and all runs included positive and non-template controls which were used for setting the cut off values. Each sample was analyzed in triplicates. In order to pass the quality check, a minimum of 10,000 droplets was required across the triplicates and a maximum of 65% of the droplets were allowed to be positive to avoid saturation. Samples without ACTB signal was excluded from further analysis. The study was performed unblinded, but project numbers were used throughout the project and cancer status not implemented until the final analysis step.

Statistical analysis

All statistical tests and graphics were performed by Stata version 14 or GraphPad, Prism version 6. Medians are presented with range. Group comparisons was performed using the Mann-Whitney U test with a two-sided P value less than 0.05 regarded significant. Survival analyses were performed using the Kaplan-Meier method. Kaplan-Meier curves were generated using publicly available microarray datasets of human lung adenocarcinoma (35) (kmplot.com/analysis). Patients were divided according to the median expression of the target gene and by stage. The following probes were used for analysis: cGAS (MB21D1) 1559051_s_, STING(TMEM173) 224929_, IFI16 206332_s_, TBK1 218520_at, IRF3 202621_at.

Results

Divergent cGAS-STING pathway functionality in NSCLC cell lines

The cGAS-STING pathway has been described to be defective within several cancer types (17-20). Thus, we initially investigated the cGAS-STING pathway expression and function in a panel of 11 NSCLC cell lines. Importantly, the gene expression analysis of cGAS, IFI16, STING, TBK1 and IRF3 showed large variation among the cell lines (*Figure 1A*,*B*,*C*,*D*,*E*). Interestingly, in four cells lines (A427, A549, H1993 and H1568) STING expression on both mRNA and protein level were undetectable (*Figure 1C*,*F*). However, five cell lines (H1975, H2228; H1650, H358 and H596) expressed STING protein at detectable levels and these cell lines were used for further analysis. Of the five cell lines only four were able to induce IFN I response (*Figure 1G*) and only three induced CCL5 (*Figure 1H*) after DNA stimulation. A similar picture was seen for stimulation with poly I:C, which is sensed through the RIG-I pathway though also dependent on TBK1 and IRF3 (*Figure 1I*,*J*). From detailed immunoblotting analysis, it was apparent that STING-dependent activation, measured by the level of phosphorylation of STING and TBK1, was acquired in all cells but to a differing degree. However, the degree of IRF3 phosphorylation and total expression did not correspond to the cytokine expression levels measured. This was clearly seen for H2228 and H596 (*Figure 1K*). Generally, the cell line H2228 which express all essential proteins relevant for an active STING pathway seems to be selective defective in the immunological response compared to for example H596 when comparing a broader range of cytokines (*Figure 1L*,*M*).

In conclusion, from these *in vitro* data it is clear that the cGAS-STING pathway is not generically defective across all NSCLC cell lines, but that there is a large window of functionality and genetically differences in the pathway, which would affect the cells capacity to mount an inflammatory cytokine response.

cGAS-STING pathway expression in NSCLC patients

Based on the results from the cell lines, we turned to investigate the clinical importance of the cGAS-STING

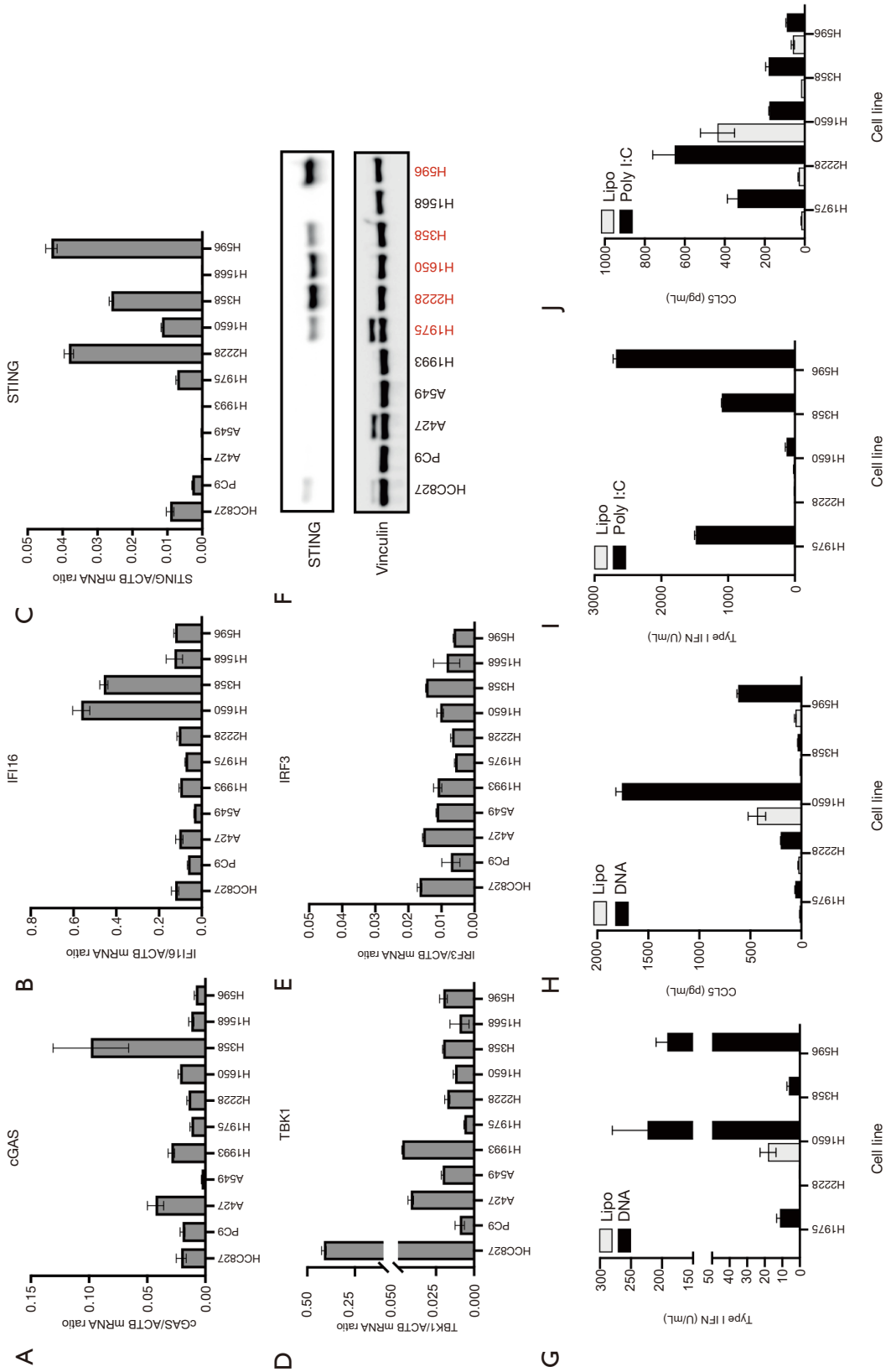

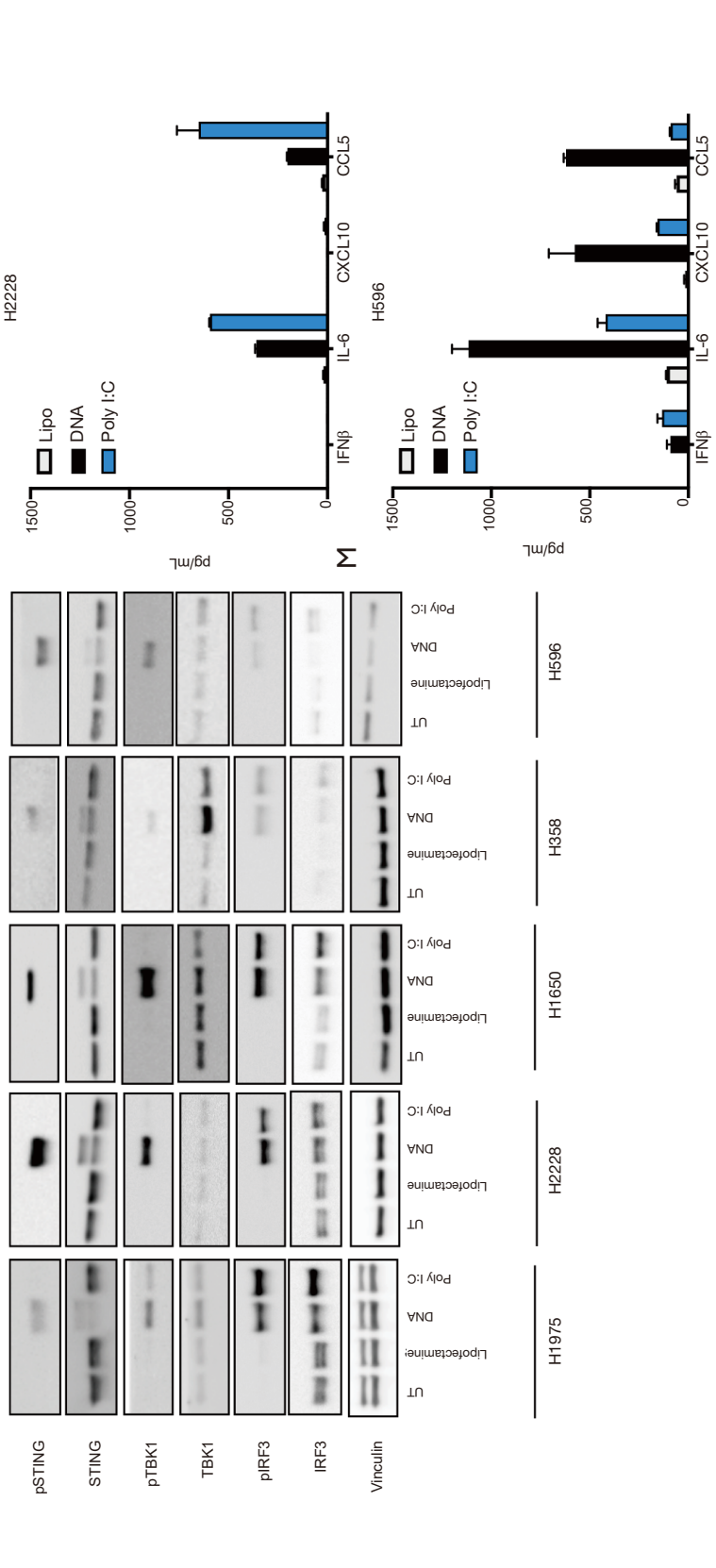

Figure 1 cGAS-STING pathway expression analysis of 11 NSCLC cell lines. (A,B,C,D,E) Gene expression analysis measured with ddPCR and normalized to ACTB; (F) immunoblotting analysis of protein expression, IFN and CCL5 response to DNA stimulation (G,H) or Poly I:C (I,J) after 20 hrs; (K) phosphoprotein analysis of cGAS-STING pathway targets after 6 hrs of stimulation with lipofectamine, DNA or Poly I:C, multiplex ELISA analysis of H2228 (L) and H596 (M). NSCLC, non-small cell lung cancer; ddPCR, droplet digital polymerase chain reaction; ACTB, actin beta; IFN I, type I interferon; Poly I:C, RIG-I agonist; Lipo, lipofectamine.

Table 1 Patient characteristics

Characteristics	Lung cancer patients (n=80)	Non-cancer patients (n=45)
Age, median [range]	67 [31–89]	62 [33–84]
Sex, n [%]		
Male	33 [41]	26 [58]
Female	47 [59]	19 [42]
Stage, n [%]		
I	20 [25]	
II	17 [21]	
III	20 [25]	
IV	23 [28]	

pathway in NSCLC. We performed gene expression analysis on a cohort of 80 NSCLC patients of all stages (*Table 1*). As it has been suggested that some tumor types epigenetically silence genes in the STING-pathway, we also included—in addition to tumor biopsies—RNA samples from matched normal tissue biopsies (n=55) and PBMCs (n=61) when obtainable (*Table 1*). For comparison, we included similar biopsies from 45 non-cancerous patients.

STING expression is increased in cancer lesions

First, we wanted to investigate whether the expression of key components in the cGAS-STING pathway was differentially expressed in NSCLC patients compared to non-cancerous patients as reported for other solid cancer types (17-19). Due to limited material from biopsies, the analysis focused on cGAS, STING and IFI16, since these are the entry of the pathway (*Figure 2A*,*B*,*C* and Figure S1A,B,C). Interestingly, we saw an increase in *STING* expression in samples from tumor biopsies compared to biopsies from non-cancer patients (*Figure 2A*). Of note, *STING* expression was generally low in non-cancer biopsies, indicating that STING is not normally highly expressed in the investigated tissue. We observed no significant difference in *cGAS* and *IFI16* expression between tumor biopsies and non-cancer biopsies (*Figure 2B*,*C*). Next, within cancer patients, we compared *STING* expression between cancer biopsies and non-cancer biopsies. Here, we observed an increased expression in the cancer lesions (*Figure 1A*). *STING* expression in non-cancer biopsies from cancer patients was, however, still elevated compared to biopsies from non-cancer patients (Figure S1A and *Figure 2A*). This could be caused by infiltrating immune cells expressing *STING* or an overall higher level of IFN I leading to increased *STING* expression.

To extend the investigation to include analysis of the patients' intrinsic cGAS-STING pathway functionality, we next investigated the gene expression levels in PBMCs for patients with available samples (cancer n=61, non-cancer n=25) (*Figure 2D*,*E*,*F*,*G*,*H*). In addition, we included *IRF3* and *TBK1* in the analysis (*Figure 2G*,*H*). Here, we observed superior expression of *cGAS* in PBMCs from non-cancer patients (*Figure 2E*), whereas no difference was observed for *STING*, *IFI16*, *IRF3* or *TBK1* expression (*Figure 2D*,*F*,*G*,*H*).

cGAS-STING pathway expression is decreased in patients with metastatic disease

cGAS-STING pathway expression has been reported to be stage-dependent with decreasing expression in tumor tissues from patients with later stage disease (19,20). To investigate this phenomenon in lung cancer, we compared gene expression of *STING*, *cGAS* and *IFI16* between patients with localized disease (stage I and II) and metastatic disease (stage III and IV) in both tumor biopsies (*Figure 3A*,*B*,*C*) and PBMCs (*Figure 3D*,*E*,*F*,*G*,*H*). We found no difference when comparing *cGAS*, *STING* or *IFI16* expression in tumor biopsies (*Figure 3A*,*B*,*C*). But in PBMCs from patients with localized disease, we observed a significantly higher expression of *cGAS* (P=0.004) (*Figure 3E*) and *TBK1* (P=0.03) (*Figure 3H*). There was an increase in *STING* expression, but this was not significant (P=0.09) (*Figure 3D*). We did not observe any difference in *IFI16* or *IRF3* expression (*Figure 3F*,*G*).

Since all investigated genes contribute to the same pathway, we examined whether there was an overall tendency towards increased pathway expression in PBMCs from patients with localized disease compared to patients with metastatic disease. We divided the expression levels on the median for each of the five genes. A larger proportion of patients with localized disease had a high expression of 3–5 genes indicating an increased overall expression of the pathway in localized disease compared to patients with regional or disseminated disease (*Table 2*).

High cGAS-STING pathway expression correlates to superior survival in localized lung cancer

The correlation between high *STING*, *cGAS* and *TBK1* expression with localized disease indicates that the

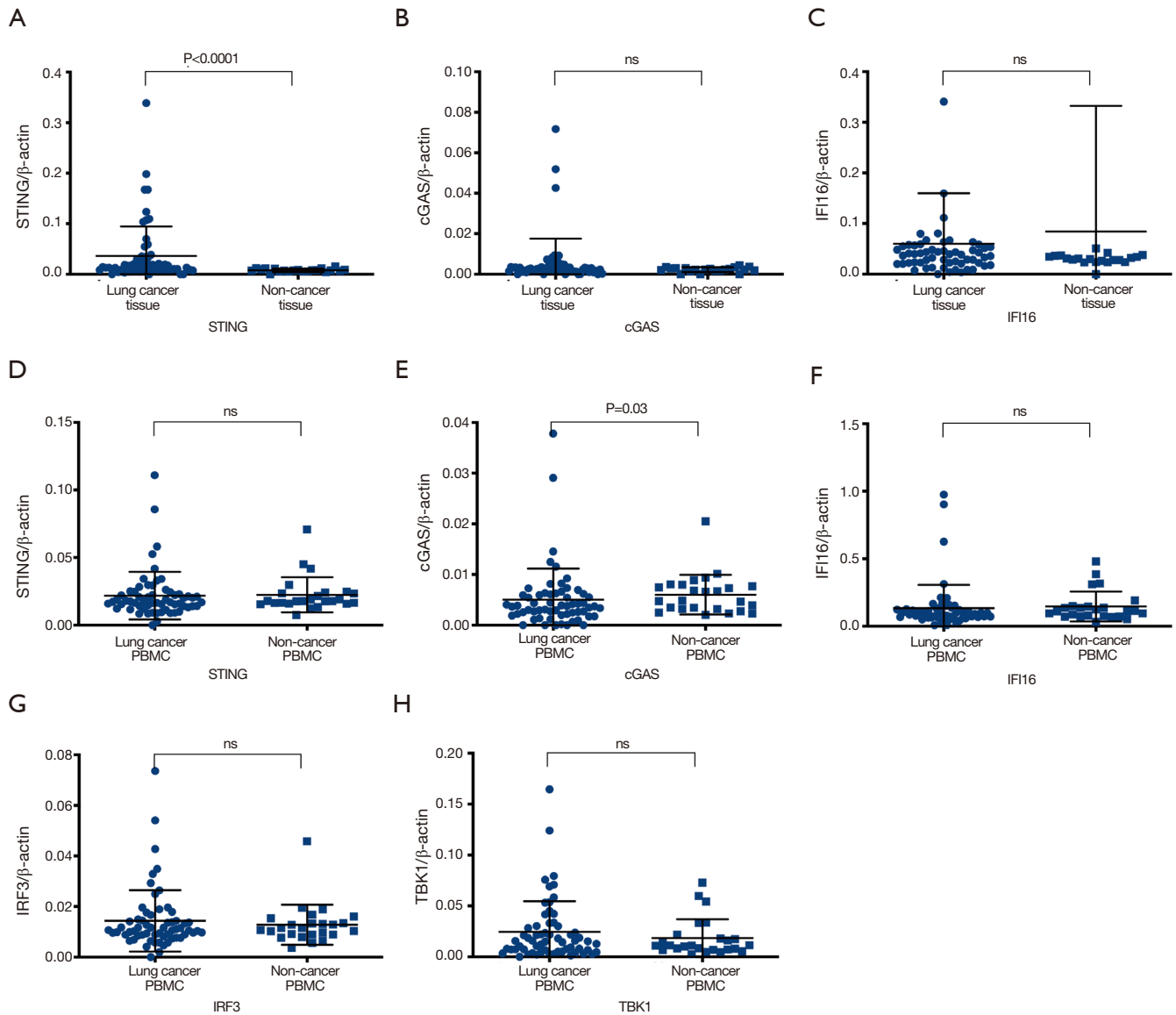

Figure 2 cGAS-STING pathway gene expression in cancer patients compared to non-cancer patients. Gene expression analysis measured with ddPCR and normalized to ACTB in (A,B,C) tumor biopsies, (D,E,F,G,H) PBMCs. Data are shown as median with range. Data was analysed with the Mann-Whitney U test and a two-sided P value P<0.05 was regarded significant. ddPCR, droplet digital polymerase chain reaction; ACTB, actin beta; PBMC, peripheral blood mononuclear cell; ns, non-significant.

expression levels of the cGAS-STING pathway may be of prognostic importance for NSCLC. In order to perform survival data analysis, we used clinical data and gene expression data from lung adenocarcinoma tumor tissue made available at KMplot.com (35) (see methods) and the results are presented in *Figure 4*. The patients were stratified by the median gene expression of *STING* (*Figure 4A,B,C,D*), *cGAS* (*Figure 4E,F,G,H*) and *TBK1* (*Figure 4I,J,K,L*) and stage. For stage I adenocarcinoma, high *STING* expression [hazard ratio (HR): 0.30 (0.19–0.47), $P=3.2\times10^{-8}$], *cGAS* expression [HR: 0.27 (0.17–0.44), $P=1.2\times10^{-8}$] and *TBK1* expression [HR: 0.33 (0.22–0.51), $P=1.5\times10^{-7}$] correlated with better OS (*Figure 4A,E,K*). Similarly, high *cGAS* [HR: 0.40 (0.23–0.70), P=0.00092] and *TBK1* [HR: 0.55 (0.34–0.90), P=0.016] expression, but not high *STING* expression was correlated with superior OS for

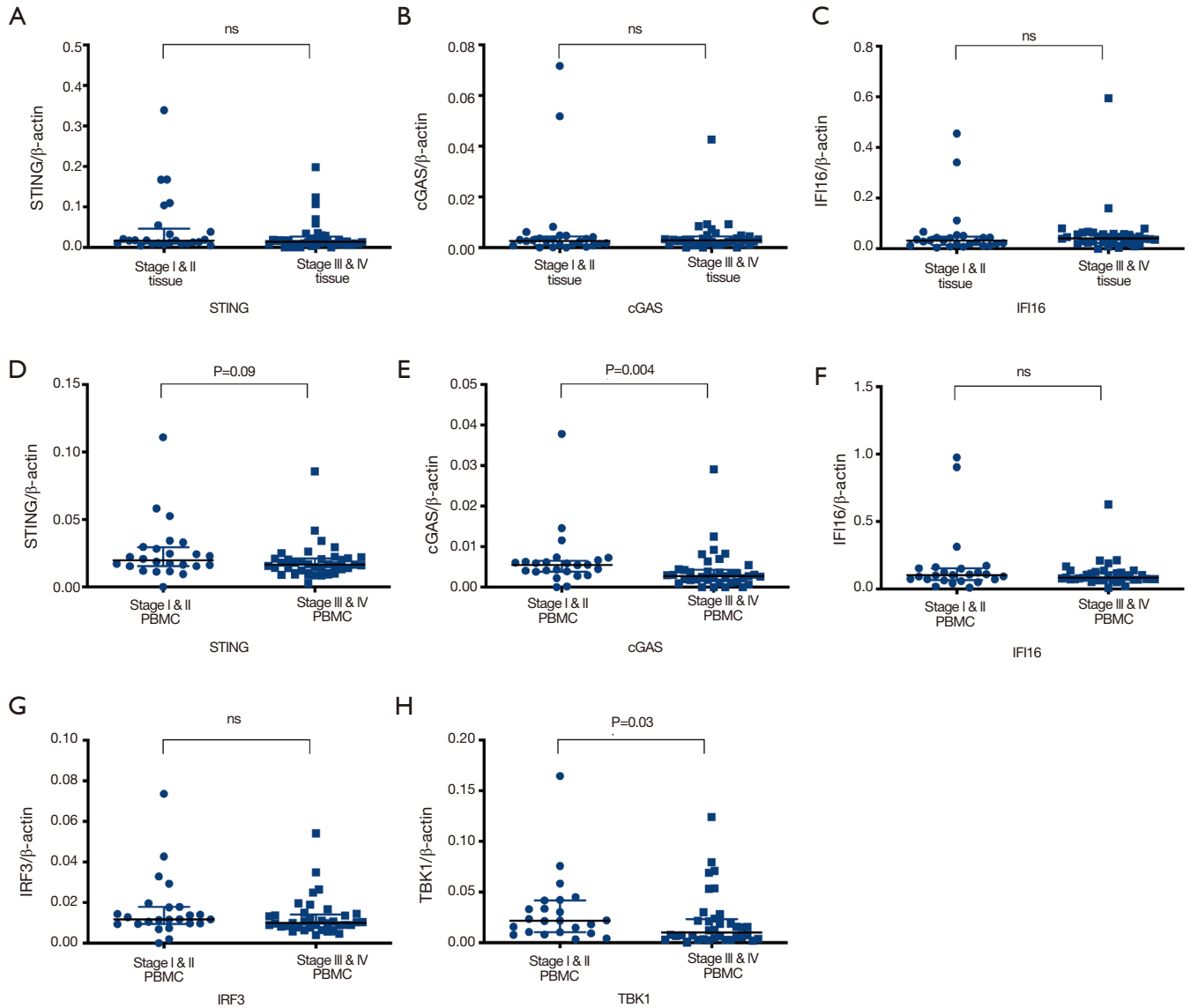

Figure 3 cGAS-STING pathway expression in localized disease (stage I & II) compared to metastatic disease (stage III & IV). Gene expression analysis measured with ddPCR and normalized to ACTB in (A,B,C) tumor biopsies, (D,E,F,G,H) PBMCs. Data are shown as median with range. Data was analyzed with the Mann-Whitney U test and a two-sided P value P<0.05 was regarded significant. ddPCR, droplet digital polymerase chain reaction; ACTB, actin beta; PBMC, peripheral blood mononuclear cell; ns, non-significant.

stage II adenocarcinoma (*Figure 4B,F,L*).

For stage III patients, there was a tendency towards high *STING* expression being correlated to inferior survival (*Figure 4C*) and there was no correlation across all stages (*Figure 4D*). For *cGAS* [HR: 0.55 (0.17–1.76), P=0.31] and *TBK1* [HR: 1.26 (0.35–3.71), P=0.67], there was no significant correlation for stage III patients (*Figure 4C,G*). Due to the low number of stage III and stage IV (four patients, not shown) patients, high *cGAS* expression was significantly correlated with better survival across all stages [HR: 0.36 (0.26–0.50), P=4.9×10^{-5}] (*Figure 4H*). There was no significant correlation for *IFI16* and *IRF3* expression

Table 2 Combined expression of cGAS-STING pathway genes

Number of genes with a high expression	Stage I & II	Stage III & IV
0–2	14	31
3–5	23	12

P=0.001.

(Figure S2A,B).

Discussion

The immune system has a pivotal role in surveilling and acting on abnormalities such as cancer within the body. In this regard, many speculates that an intact and highly functional innate immune system will have a detrimental effect on patients' capacity to establish a sufficient anti-tumoral response. In this context, it is likely that the level of activation of the cGAS-STING DNA-sensing pathway is crucial. For example in syngeneic cancer mouse models an antitumoral immunity effect of administering STING agonist intratumorally has been observed (21). Furthermore the effect of radiotherapy (37), checkpoint inhibitors (22,23,38,39) and recently PARP inhibitors (40,41) are all highly dependent on the presence of STING and the anti-cancer effects are elevated when these cancer therapies are combined with STING agonist drugs.

In a cancer setting, it is evident to investigate immune status and activation within the cancer site, but the peripheral immune system may also provide important information, especially on the intrinsic function or capacity to mount an immunological response. Our study shows that *STING* expression is increased in tumor tissue from lung adenocarcinoma patients compared to non-cancer controls. This increase in *STING* expression observed in cancer lesions may be associated with an elevated immune cell infiltration as well as a higher percentage of myeloid cells, including monocytes, macrophages and dendritic cells where the level of activation can influence the expression of *STING*. Since the tumor tissue examined in this study was obtained by FNAs, we did not have information on infiltrating immune cells nor tumor grade.

Due to limited access to biopsies from especially patients with metastatic disease, we wanted to investigate the potential for investigating cGAS-STING pathway expression in PBMCs. Here, we observed superior *cGAS* expression in PBMCs from non-cancer patients compared to cancer patients. Furthermore, we detected a significant decrease in *cGAS*, *STING* and *TBK1* expression in PBMCs from patients with metastatic disease compared to patients with localized disease in agreement with other studies on stage dependent expression, although within tumor tissue (20). The decrease in CGAS expression from non-cancer to cancer and from localized disease to late stage disease may be due to some not yet identified inherent genetic variation or due to epigenetic regulation of *cGAS* expression as previously described for tumor cells (20). Our findings based on peripheral gene expression supports a recent study reporting transcriptional changes in monocytes of cancer patients (27) and indicate a role for gene expression analysis based on PBMCs. PBMCs are highly available and not as susceptible to sampling bias, which may be seen when using fine-needle biopsies. Based on our PBMC data, expression of the cGAS-STING pathway in peripheral blood cells seems to harbor potential as a minimal invasive prognostic biomarker in localized lung adenocarcinoma.

As a function of the screening of 11 NSCLC cell lines, we found that STING, cGAS and IFI16 was heterogeneously expressed. Interestingly, in those cell lines that did express STING, we observed a large variation in response to DNA. In one cell line, the STING pathway seemed to be activated down to the level of IRF3 phosphorylation, however, the cells still did not produce IFN I, but merely various inflammatory cytokines. These data clearly show a diversity in the cGAS-STING pathway from complete non-responders to responders on different immunological levels. A diversity that may be established during tumor progression as outlines below.

Through engagement of available clinical data sets, we demonstrated that high expression of *cGAS*, *STING* and *TBK1* correlates with superior survival in lung adenocarcinoma, but most pronounced for patients with stage I and II disease. This may indicate that expression of the cGAS-STING pathway decreases the risk of recurrence and hereby recurrence-related death. A recent contradictory finding pointed to high *TBK1* expression being correlated to shorter OS in lung adenocarcinoma, but stage of disease was not considered and hence the results cannot be compared directly (42).

Contradictory, stage-dependent survival analysis revealed a tendency for high *STING* expression to correlate with inferior survival in stage III patients. Due to a low number of stage III patients, these results should be interpreted

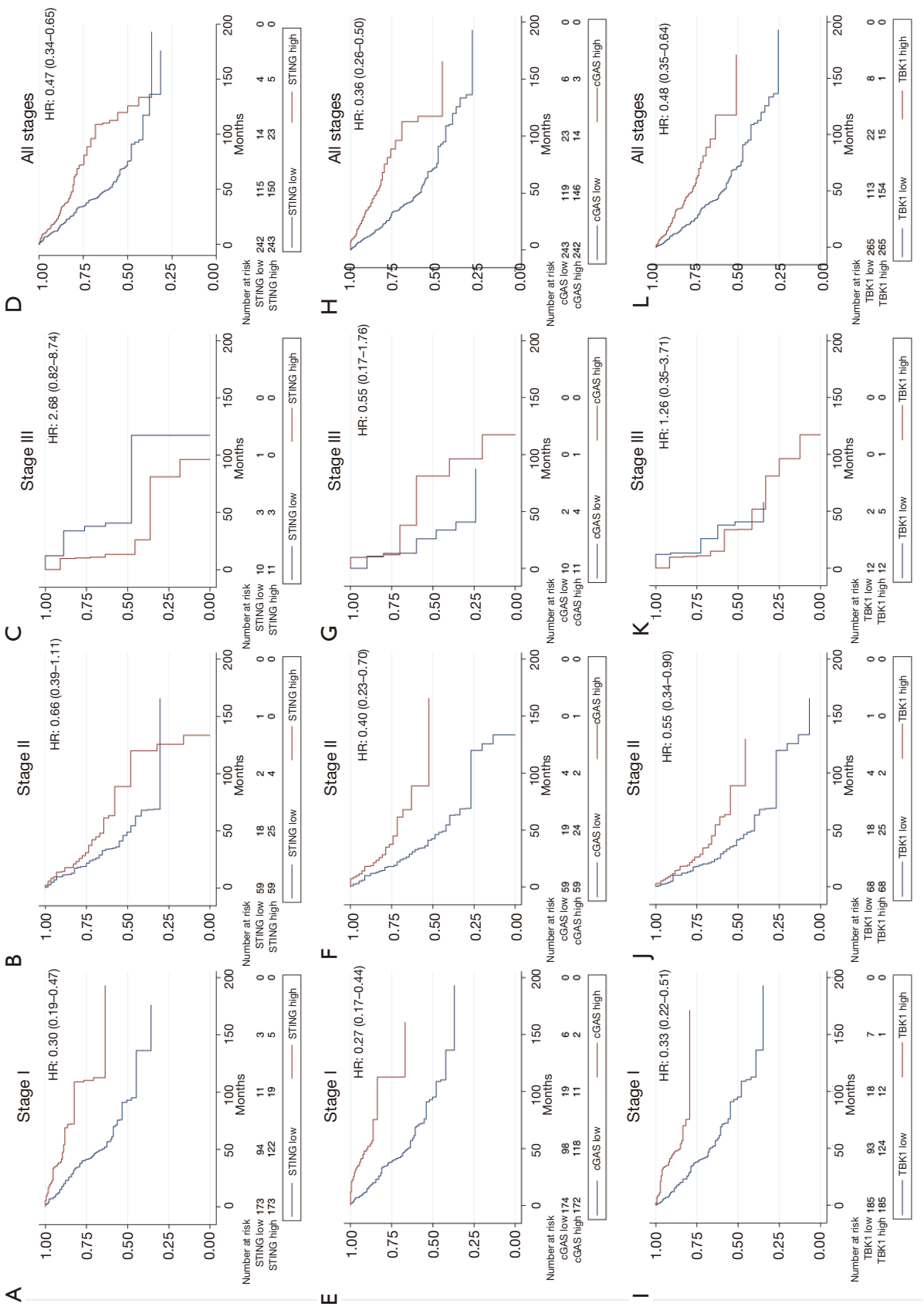

Figure 4 Kaplan-Meier survival analysis for stage I–III lung adenocarcinoma patients. The Kaplan-Meier plots was generated using gene expression data from microarray analysis and clinical data available at kmplot.com for (A,B,C,D) STING (n=485), (E,F,G,H) cGAS (n=485), (I,J,K,L) TBK1 (n=530). Patients were divided according to the median expression of the target gene. HR, hazard ratio.

with caution. Although, the finding can be explained by the proposed metastasis-promoting role of STING, where cytosolic DNA in cells with high chromatin instability drive STING-mediated metastasis through non-canonical NFκB signaling (16). In contrast, *cGAS* expression seemed to impact prognosis across all stages of lung adenocarcinoma. cGAS has been shown to inhibit cancer immortalization through a STING-independent mechanism and induce senescence upon DNA damage (25). Likely, STING has also been shown to elicit a NFκB driven inflammation response through a DNA damage repair system mechanism that is cGAS-independent (43). This may call for an important STING-independent role for cGAS in auditing cancer progression and a non-canonical STING pathway controlling cancer progression.

Since *STING* expression has been correlated to a better clinical outcome in colorectal and hepatocellular carcinoma (17,19), STING agonists have been investigated as a potential cancer treatment. The function of STING agonists is dependent on STING protein being present at a minimum basal level. Hence, our study may implicate that STING agonists have a therapeutic potential in localized disease as an adjuvant treatment. In these early stages, clinical trials have primarily tested STING agonists in a variety of patients with late-stage metastatic diseases within a broad scope of cancer types, where STING agonists may be less efficient due to stage-dependent loss of *STING* expression.

The decreased expression of STING in metastatic disease together with the known contradictory roles of STING function highlights the need for further studies on STING modulation during cancer progression. Hereby, we will be better suited to access the role and potential for STING agonist as a cancer treatment in different types and stages of cancer.

Acknowledgments

We thank Ane Kjeldsen, Department of Biomedicine, Aarhus University and Birgit Westh Mortensen, Department of Clinical Biochemistry, Aarhus University Hospital for assistance in the laboratory.

Funding: This study was partly funded by grants from Danish Cancer Society (R167-A10737-17-S2); Lundbeck foundation (R238-2016-2708), Tømrermester Jørgen Holm og hustru Elisa F. Hansens mindelegat, and Dagmar Marshalls fond.

Footnote

Reporting Checklist: The authors have completed the REMARK reporting checklist. Available at http://dx.doi.org/10.21037/tlcr-20-524

Data Sharing Statement: Available at http://dx.doi.org/10.21037/tlcr-20-524

Peer Review File: Available at http://dx.doi.org/10.21037/tlcr-20-524

Conflicts of Interest: All authors have completed the ICMJE uniform disclosure form (available at http://dx.doi.org/10.21037/tlcr-20-524). Dr. KRG reports grants from Tømrermester Jørgen Holm og hustru Elisa F. Hansens mindelegat and from Dagmar Marshalls Foundation during the conduct of the study; Dr. MRJ reports receiving research grants from The Lundbeck foundation and Danish Cancer Society during the conduct of the study. Furthermore, Dr. MRJ is scientific founder of and part-time CSO at Stipe Therapeutics. The other authors have no conflicts of interest to declare.

Ethical Statement: The authors are accountable for all aspects of the work in ensuring that questions related to the accuracy or integrity of any part of the work are appropriately investigated and resolved. The study was conducted in accordance with the declaration of Helsinki (as revised in 2013). The study was approved by The Central Denmark Region Committees on Biomedical Research Ethics (M-20100246) and the Danish Agency of Data Protection (1-16-02-346-14). All patients gave informed written consent before inclusion and individual consent for this retrospective analysis was waived.

References

1. Rosenthal R, Cadieux EL, Salgado R, et al. Neoantigen-directed immune escape in lung cancer evolution. Nature 2019;567:479-85.
2. Balachandran VP, Łuksza M, Zhao JN, et al. Identification of unique neoantigen qualities in long-term survivors of pancreatic cancer. Nature 2017;551:512-6.
3. Cristescu R, Mogg R, Ayers M, et al. Pan-tumor genomic biomarkers for PD-1 checkpoint blockade-based immunotherapy. Science 2018;362:eaar3593.
4. Patel SJ, Sanjana NE, Kishton RJ, et al. Identification of essential genes for cancer immunotherapy. Nature 2017;548:537-42.
5. Siegel RL, Miller KD, Jemal A. Cancer statistics, 2018. CA Cancer J Clin 2018;68:7-30.
6. Uramoto H, Tanaka F. Recurrence after surgery in patients with NSCLC. Transl Lung Cancer Res 2014;3:242-9.
7. Burotto M, Thomas A, Subramaniam D, et al. Biomarkers in early-stage non-small-cell lung cancer: current concepts and future directions. J Thorac Oncol 2014;9:1609-17.
8. Jain P, Jain C, Velcheti V. Role of immune-checkpoint inhibitors in lung cancer. Ther Adv Respir Dis 2018;12:1753465817750075.
9. Suzuki K, Kachala SS, Kadota K, et al. Prognostic immune markers in non-small cell lung cancer. Clin Cancer Res 2011;17:5247-56.
10. Bryant CM, Albertus DL, Kim S, et al. Clinically relevant characterization of lung adenocarcinoma subtypes based on cellular pathways: an international validation study. PLoS One 2010;5:e11712.
11. Sokol CL, Luster AD. The chemokine system in innate immunity. Cold Spring Harb Perspect Biol 2015;7:a016303.
12. Harding SM, Benci JL, Irianto J, et al. Mitotic progression following DNA damage enables pattern recognition within micronuclei. Nature 2017;548:466-70.
13. Sun L, Wu J, Du F, et al. Cyclic GMP-AMP synthase is a cytosolic DNA sensor that activates the type I interferon pathway. Science 2013;339:786-91.
14. He L, Xiao X, Yang X, et al. STING signaling in tumorigenesis and cancer therapy: A friend or foe? Cancer Lett 2017;402:203-12.
15. Schneider WM, Chevillotte MD, Rice CM. Interferon-stimulated genes: a complex web of host defenses. Annu Rev Immunol 2014;32:513-45.
16. Bakhoum SF, Ngo B, Laughney AM, et al. Chromosomal instability drives metastasis through a cytosolic DNA response. Nature 2018;553:467-72.
17. Yang CA, Huang HY, Chang YS, et al. DNA-sensing and nuclease gene expressions as markers for colorectal cancer progression. Oncology 2017;92:115-24.
18. Song S, Peng P, Tang Z, et al. Decreased expression of STING predicts poor prognosis in patients with gastric cancer. Sci Rep 2017;7:39858.
19. Bu Y, Liu F, Jia QA, et al. Decreased expression of TMEM173 predicts poor prognosis in patients with hepatocellular carcinoma. PLoS One 2016;11:e0165681.
20. Xia T, Konno H, Barber GN. Recurrent loss of STING signaling in melanoma correlates with susceptibility to viral oncolysis. Cancer Res 2016;76:6747-59.
21. Ager CR, Reilley MJ, Nicholas C, et al. Intratumoral STING activation with T-cell checkpoint modulation generates systemic antitumor immunity. Cancer Immunol Res 2017;5:676-84.
22. Jing W, McAllister D, Vonderhaar EP, et al. STING agonist inflames the pancreatic cancer immune microenvironment and reduces tumor burden in mouse models. J Immunother Cancer 2019;7:115.
23. Foote JB, Kok M, Leatherman JM, et al. A STING agonist given with OX40 receptor and PD-L1 modulators primes immunity and reduces tumor growth in tolerized mice. Cancer Immunol Res 2017;5:468-79.
24. Ding L, Huang XF, Dong GJ, et al. Activated STING enhances Tregs infiltration in the HPV-related carcinogenesis of tongue squamous cells via the c-jun/CCL22 signal. Biochim Biophys Acta 2015;1852:2494-503.
25. Yang H, Wang H, Ren J, et al. cGAS is essential for cellular senescence. Proc Natl Acad Sci 2017;114:E4612-20.
26. Della Corte CM, Sen T, Gay CM, et al. STING pathway expression identifies non-small cell lung cancers with an immune-responsive phenotype. J Thorac Oncol 2020;15:777-91.
27. Cassetta L, Fragkogianni S, Sims AH, et al. Human tumor-associated macrophage and monocyte transcriptional landscapes reveal cancer-specific reprogramming, biomarkers, and therapeutic targets. Cancer Cell 2019;35:588-602.e10.
28. Jønsson KL, Laustsen A, Krapp C, et al. IFI16 is required for DNA sensing in human macrophages by promoting production and function of cGAMP. Nat Commun 2017;8:14391.
29. Sandfeld-Paulsen B, Aggerholm-Pedersen N, Bæk R, et al.

Exosomal proteins as prognostic biomarkers in non-small cell lung cancer. Mol Oncol 2016;10:1595-602.
30. Jakobsen KR, Paulsen BS, Bæk R, et al. Exosomal proteins as potential diagnostic markers in advanced non-small cell lung carcinoma. J Extracell Vesicles 2015;4:26659.
31. Sandfeld-Paulsen B, Jakobsen KR, Bæk R, et al. Exosomal proteins as diagnostic biomarkers in lung cancer. J Thorac Oncol 2016;11:1701-10.
32. Sandfeld-Paulsen B, Holst Folkersen B, Riis Rasmussen T, et al. Gene expression of the EGF System-a prognostic model in non-small cell lung cancer patients without activating EGFR mutations 1. Transl Oncol 2016;9:306-12.
33. Sandfeld-Paulsen B, Meldgaard P, Aggerholm-Pedersen N. Comorbidity in lung cancer: a prospective cohort study of self-reported versus register-based comorbidity. J Thorac Oncol 2018;13:54-62.
34. Sandfeld-Paulsen B, Meldgaard P, Sorensen BS, et al. The prognostic role of inflammation-scores on overall survival in lung cancer patients. Acta Oncol 2019;58:371-6.
35. Nagy Á, Lánczky A, Menyhárt O, et al. Validation of miRNA prognostic power in hepatocellular carcinoma using expression data of independent datasets. Sci Rep 2018;8:9227.
36. Sandfeld-Paulsen B, Demuth C, Folkersen BH, et al. Ultra-micro samples can be used for mRNA quantification of lung cancer biomarkers. Scand J Clin Lab Invest 2016;76:243-8.
37. Deng L, Liang H, Xu M, et al. STING-dependent cytosolic DNA sensing promotes radiation-induced type I interferon-dependent antitumor immunity in immunogenic tumors. Immunity 2014;41:843-52.
38. Sivick KE, Desbien AL, Glickman LH, et al. Magnitude of therapeutic STING activation determines CD8+ T cell-mediated anti-tumor immunity. Cell Rep 2018;25:3074-85.e5.
39. Kinkead HL, Hopkins A, Lutz E, et al. Combining STING-based neoantigen-targeted vaccine with checkpoint modulators enhances antitumor immunity in murine pancreatic cancer. JCI Insight 2018;3:e122857.
40. Ding L, Kim HJ, Wang Q, et al. PARP Inhibition elicits STING-dependent antitumor immunity in brca1-deficient ovarian cancer. Cell Rep 2018;25:2972-80.e5.
41. Pantelidou C, Sonzogni O, Taveira MDO, et al. Parp inhibitor efficacy depends on CD8+ T-cell recruitment via intratumoral sting pathway activation in brca-deficient models of triple-negative breast cancer. Cancer Discov 2019;9:722-37.
42. An X, Zhu Y, Zheng T, et al. An analysis of the expression and association with immune cell infiltration of the cGAS/STING pathway in pan-cancer. Mol Ther Nucleic Acids 2019;14:80-9.
43. Dunphy G, Flannery M, Almine JF, et al. Non-canonical activation of the DNA sensing adaptor STING by ATM and IFI16 mediates NF-κB signaling after nuclear DNA damage. Mol Cell 2018;71:745-60.

Cite this article as: Raaby Gammelgaard K, Sandfeld-Paulsen B, Godsk SH, Demuth C, Meldgaard P, Sorensen BS, Jakobsen MR. cGAS-STING pathway expression as a prognostic tool in NSCLC. Transl Lung Cancer Res 2021;10(1):340-354. doi: 10.21037/tlcr-20-524

